Full counting statistics of Andreev reflection: Signatures of a quantum transition

G. C. Duarte-Filho and A. M. S. Macêdo
Departamento de Física, Laboratório de Física Teórica e Computacional, Universidade Federal de Pernambuco, 50670-901 Recife, PE, Brazil

(Received 17 March 2009; revised manuscript received 26 June 2009; published 20 July 2009)

Employing semiclassical circuit theory, we study the charge-transfer statistics of a quantum dot (chaotic cavity) connected to a normal metal and a superconducting reservoir via two non-ideal barriers. We assume the absence of a magnetic field and a low-energy regime so that the energy dependence of the Andreev reflection eigenvalues can be neglected. We calculate analytically the first three charge-transfer cumulants and the density of Andreev reflection eigenvalues. We observe an interesting signature in the charge-transfer cumulants of a quantum transition that takes place in the chaotic cavity [A. M. S. Macêdo and A. M. C. Souza, Phys. Rev. E **71**, 066218 (2005)] associated with the formation of Fabry-Perot modes. Our results compare well with numerical simulations obtained from the scattering matrix formalism.

DOI: 10.1103/PhysRevB.80.035311 PACS number(s): 73.21.La

I. INTRODUCTION

Hybrid normal-metal-superconductor (NS) mesoscopic devices are important model systems in which to study the interplay between normal metal phase-coherent phenomena and superconductor-induced proximity effects. Observed phenomena in these devices build on the underlying microscopic mechanism of conversion of an electron-hole quasiparticle pair in the metallic terminal onto a Cooper pair in the superconductor. The conversions take place at the NS interface via Andreev reflections.[1]

An efficient way to describe charge transport in a mesoscopic device is to study its full counting statistics (FCS),[2] which amounts to determining the probability, $P_n(T_0)$, that n units of charge are transferred during the observation time T_0. The value of $P_n(T_0)$ depends both on quantum-mechanical uncertainties of the transmission process and on the Pauli principle. A typical mesoscopic device consists of a phase-coherent conductor connected to two metallic reservoirs. It is convenient to characterize the mesoscopic conductor via its set of transmission eigenvalues $\{\tau_j\}$, i.e., the eigenvalues of $tt^\dagger$, where t is the transmission matrix. The FCS of the mesoscopic conductor is fully characterized by specifying the characteristic function $e^{M_0\Phi(\lambda)} \equiv \Sigma_n P_n(T_0) e^{in\lambda}$, where $M_0 = eVT_0/h$ is the number of transmission attempts per channel, and V is the voltage applied through the sample. At zero-temperature $\Phi(\lambda)$ describes independent binomial processes

$$\Phi(\lambda) = \sum_{j=1}^{N} \ln[1 + \tau_j(e^{i\lambda} - 1)]. \tag{1}$$

Transport observables are given simply by derivatives of $\Phi(\lambda)$ at $\lambda = 0$. The dimensionless conductance and shot-noise power, e.g., are given, respectively, by $g = -i\Phi'(0) = \Sigma_j \tau_j$ and $p = -\Phi''(0) = \Sigma_j \tau_j(1-\tau_j)$. In the presence of chaotic scattering random matrix theory predicts that the transmission eigenvalues of the mesoscopic conductor become correlated random variables and consequently $\Phi(\lambda)$ fluctuates, thus making it an incomplete characterization of the charge transport process. In the semiclassical regime, defined by a large number of open channels $N \gg 1$, we may neglect these fluctuations and describe $\Phi(\lambda)$ by means of a circuit theory.[3]

In NS hybrid structures the charge transport statistics is conveniently described at energies much lower than the Thouless energy and in the absence of a magnetic field in terms of Andreev reflection eigenvalues $\{r_j\}$, i.e., the eigenvalues of $s_{eh}s_{eh}^\dagger$, where s_{eh} is the Andreev reflection matrix. The corresponding characteristic function, denoted $\Phi_{NS}(\lambda)$, is given by Eq. (1) with Andreev reflection eigenvalues $\{r_j\}$ replacing the transmission eigenvalues $\{\tau_j\}$. The dimensionless conductance and shot-noise power read $g_{NS} = -i\Phi'_{NS}(0) = \Sigma_j r_j$ and $p_{NS} = -\Phi''_{NS}(0) = \Sigma_j r_j(1-r_j)$, respectively. There is a simple relation between Andreev reflection eigenvalues and transmission eigenvalues, given by $r_j = \tau_j^2/(2-\tau_j)^2$, which can be used to calculate transport observables of NS systems using the statistical properties of transmission eigenvalues.[4]

An important feature of NS structures is the appearance of a transport regime denominated *reflectionless tunneling*,[5] in which there is a gradual transition from two-particle to single-particle tunneling as one lowers the transparency of the NS interface. If the mesoscopic conductor consists of a difusive metal the reflectionless tunneling regime is associated with disorder-induced openings of tunneling channels,[5,6] i.e., the emergence of transmission eigenvalues close to one. A similar effect occurs in a double-barrier junction,[7] if one varies the transparency of one barrier while keeping the other fixed. The model used in Ref. 7 contains the assumption of non-overlapping transmission resonances with independent random-phase shifts, which is not appropriate for ballistic chaotic cavities. A more flexible model is obtained by using Nazarov's circuit theory.[6,8] Using this approach, Vanević and Belzig[9] studied the first three FCS cumulants of an NS system composed of a quantum dot ideally coupled to asymmetric leads. The energy dependence of the average density of Andreev eigenvalues was studied in Ref. 10 using a circuit-theory-like quasiclassical Green's-function approach. They found that at energies on the order of the Thouless energy, the proximity effect causes the opening up of resonant particle-hole channels, i.e., the emergence of Andreev reflection eigenvalues close to unit.

The opening up of resonant transmission channels, upon varying the transparencies of a double-barrier chaotic ballistic cavity, was studied in Ref. 11, where it was interpreted as a quantum transition associated with the emergence of Fabry-Perot resonances inside the cavity. Although it can be easily seen in the average density of transmission eigenvalues in the semiclassical limit, it does not show up in any of the FCS cumulants, thus making it hard to observe experimentally. There has been two proposals of signatures of this transition in observable quantities. In the first one[12] the system is embedded in an electromagnetic environment, which emulates a weak Coulomb interaction, and the transition can be seen in the Fano factor at low temperatures and low voltages. In the second proposal[13] a signature of the transition is shown to appear in the low-transmission tail of the transmitted charge distribution.

In this work we study the quantum transition in the presence of the proximity effect. Using a scalar version of circuit theory, we calculate the first three cumulants of charge-transfer statistics of an NS system that consists of a ballistic chaotic cavity coupled via barriers of arbitrary transparencies to a normal metal and a superconducting reservoir. We verify that all three cumulants show distinctive features around the transition lines. These results agree well with independent numerical simulations. This paper is organized as follows: in Sec. II we present a formulation of the generating function of FCS in our NS systems as a scalar circuit theory, thus extending the formalism presented in Ref. 14. In Sec. III the scheme is used to calculate the average density of Andreev reflection eigenvalues. Two cases with simple analytical solutions (a chaotic cavity with symmetric barriers and one with tunnel junctions) are discussed before a more complex case (a chaotic cavity with an ideal contact and a barrier of arbitrary transparency) is considered. Through the analysis of the average density of Andreev reflection eigenvalues in the latter case we show the emergence of the reflectionless tunneling regime as we vary the transparency of the barrier. In Sec. IV the general case of a chaotic cavity with two barriers of arbitrary transparencies are presented. We compute the first three FCS cumulants and verify that such observables exhibit a signature of the quantum phase transition as we vary the barriers transparencies. Results for the Fano Factor and the Skewness, defined as the ratio between the third and the first cumulants, are also presented. Finally, the average density of Andreev reflection eigenvalues are calculated and we are able to observe the emergence of resonant channels with eigenvalues close to one upon varying the transparencies of the barriers. A summary and conclusions are presented in Sec. V.

II. CIRCUIT THEORY AND FCS

In this section we present a circuit-theory approach to calculate the generating function of charge-transfer statistics of an NS device. We start by writing the FCS generating function in terms of Andreev reflection eigenvalues $\{r_j\}$ as follows:

$$\Phi_{NS}(\lambda) = \sum_{j=1}^{N} \ln[1 + r_j(e^{i\lambda} - 1)]. \tag{2}$$

We assume low temperature and low voltage so that $\max(eV, k_BT) \ll \min(E_{Th}, |\Delta|)$, where E_{Th} is the Thouless energy and Δ is the superconducting order parameter. Under this condition we can neglect the energy dependence of the scattering matrices and thus the Andreev reflection eigenvalues r_j are also energy independent. In the presence of chaotic scattering the eigenvalues $\{r_j\}$ become random and correlated, so that we may introduce the average generating function

$$S(\lambda) \equiv \langle \Phi(\lambda) \rangle = \int_0^1 dr \rho_{NS}(r) \ln[1 + r(e^{i\lambda} - 1)], \tag{3}$$

where $\rho_{NS}(r) = \Sigma_n \langle \delta(r - r_n) \rangle$ is the average density of Andreev reflection eigenvalues. In the semiclassical regime, characterized by a large number of open scattering channels $N \gg 1$, $\rho_{NS}(r)$ becomes a well-behaved smooth function. With this in mind, we define the following auxiliary function

$$g_{NS}(\varepsilon) = -i \left. \frac{\partial S(\lambda)}{\partial \lambda} \right|_{e^{i\lambda} = 1 - \varepsilon^2} = \int_0^1 dr \rho_{NS}(r) \frac{(1 - \varepsilon^2) r}{1 - \varepsilon^2 r}. \tag{4}$$

Using $g_{NS}(\varepsilon)$ the FCS cumulants can be obtained through the formula

$$q_{l+1} = \left(\frac{\varepsilon^2 - 1}{2\varepsilon} \frac{d}{d\varepsilon} \right)^l g_{NS}(\varepsilon)|_{\varepsilon = 0}; \quad l = 0, 1, \ldots . \tag{5}$$

It is also convenient to introduce the following change in variables, $r = \mathrm{sech}^2 x$, and define the new average density $\nu_{NS}(x)$, which is obtained from $g_{NS}(\varepsilon)$ through

$$\nu_{NS}(x) = \frac{2}{\pi} \mathrm{Im} \left\{ \frac{i\varepsilon}{\sqrt{1 - \varepsilon^2}} g_{NS}(\varepsilon)|_{\varepsilon = \cosh x} \right\}. \tag{6}$$

The density $\nu_{NS}(x)$ is directly related to $\rho_{NS}(r)$ via the transformation formula

$$\rho_{NS}(r) = \frac{\nu_{NS}[\cosh^{-1}(1/\sqrt{r})]}{2r\sqrt{1 - r}}. \tag{7}$$

Let us now formulate the calculation of $g_{NS}(\varepsilon)$ as a problem in circuit theory. We start by defining the function

$$F(\phi) \equiv \int_0^1 d\tau \frac{\tau \rho(\tau)}{1 - \tau \sin^2 \phi/2}, \tag{8}$$

where $\rho(\tau) = \Sigma_n \langle \delta(\tau - \tau_n) \rangle$ is the average density of transmission eigenvalues. One can express $g_{NS}(\varepsilon)$ in terms of $F(\phi)$ as follows:

$$g_{NS}(\varepsilon) = -\frac{1 - \varepsilon^2}{4\varepsilon} [F_+(\varepsilon) - F_-(\varepsilon)], \tag{9}$$

where

$$F_{\pm}(\varepsilon) = F(\phi)\big|_{\sin^2\phi/2=(1-\varepsilon^2)/[2(1\pm\varepsilon)]}. \tag{10}$$

The main advantage of the circuit-theory approach is the fact that $F(\phi)$ can be calculated directly without having to calculate $\rho(\tau)$ first.

Our presentation of quantum circuit theory will be brief, for a more detailed description we recommend Refs. 3, 6, 8, and 14. A central concept in circuit theory is the pseudocurrent defined as $I(\phi) \equiv \sin\phi F(\phi)$, in which ϕ plays the role of a pseudopotential. To be specific, we consider a mesoscopic system consisting of a ballistic chaotic cavity coupled via barriers of arbitrary transparencies to two electron reservoirs. In circuit-theory language the reservoirs and the cavity are represented as terminals and nodes, respectively, with associated pseudopotentials. The basic circuit-theory equation for this system is the conservation law for the pseudocurrent

$$I(\phi) = I_1(\phi - \theta) = I_2(\theta). \tag{11}$$

In circuit theory the barriers play the role of connectors whose "current-voltage" relations are given by

$$I_j(\Delta\phi_j) = \frac{2N_jT_j\tan(\Delta\phi_j/2)}{1+(1-T_j)\tan^2(\Delta\phi_j/2)}; \quad j=1,2, \tag{12}$$

where N_j denotes the number of open scattering channels in the j-th connector, T_j is the connector's transparency, and $\Delta\phi_j$ represents the pseudopotential drop along the connector. The basic problem is the determination of the pseudopotential θ at the central node. Defining the variable $\xi=\tan\theta/2$ we can rewrite the second equality of Eq. (11) as the following polynomial equation:

$$\begin{aligned} &T_1(1-T_2)\eta\xi^4 + (1+2a)T_1T_2\eta\xi^2 \\ &\quad + [\{[aT_2 - T_1(1-T_2)]\eta^2 + aT_2(1-T_1) + T_1(1-T_2)\}]\xi^3 \\ &\quad + \{[aT_2(1-T_1) - T_1]\eta^2 + T_1 + aT_2\}\xi - T_1\eta = 0, \end{aligned} \tag{13}$$

where $\eta=\tan\phi/2$ and $a=N_2/N_1$. With the solution to this equation we compute $F(\phi)$ and finally obtain $g_{NS}(\varepsilon)$ via the relation

$$g_{NS}(\varepsilon) = \frac{\sqrt{1-\varepsilon^2}}{2\varepsilon}\left(\frac{N_2T_2\xi_-}{1+(1-T_2)\xi_-^2} - \frac{N_2T_2\xi_+}{1+(1-T_2)\xi_+^2}\right), \tag{14}$$

where $\xi_{\pm}$ is the physical solution of Eq. (13) with η chosen as $\eta_{\pm}=\sqrt{(1\mp\varepsilon)/(1\pm\varepsilon)}$.

In the next section we shall use $g_{NS}(\varepsilon)$ to calculate the average density of Andreev reflection eigenvalues. This quantity displays a clear signature of the quantum transition reported in Ref. 11 as we vary the barriers transparencies.

III. AVERAGE DENSITY OF ANDREEV REFLECTION EIGENVALUES

We begin this section by treating two simple cases in which we can compute very simple analytical expressions for $\rho_{NS}(r)$ using circuit theory. The first system is a chaotic cavity with symmetric barriers, so that $T_1=T_2=T$. With this simplification Eq. (13) factorizes and the physical root can be obtained from the following quadratic equation:

$$a\eta\xi^2 + (1+a)\xi - \eta = 0 \tag{15}$$

Inserting the physical root into Eq. (14) we obtain $g_{NS}(\varepsilon)$, which we use to calculate $\nu(x)$ via Eq. (6). Finally, from Eq. (7) we derive $\rho_{NS}(r)$ which reads

$$\rho_{NS}^{\mathrm{sym}}(r) = \frac{N}{\pi}\frac{T(1+\sqrt{r})}{\sqrt{r(1-r)}}\Xi(r), \tag{16}$$

where $\Xi(r)$ is a well-behaved function at $r=0$ and $r=1$, which is given by

$$\Xi(r) = \frac{(2+T)\alpha + (2-7T)r}{[T\alpha + (8-7T)r]^2 + 16r(\alpha-3r)}, \tag{17}$$

where $\alpha=(1+2\sqrt{r})$. Note in Eq. (16) the presence of inverse square-root singularities for r close to both one and zero.

The other simple case is that of a chaotic cavity with two tunnel junctions, i.e., barriers of transparencies that are much smaller than one ($T_1, T_2 \ll 1$). In this tunnel junction regime the average density $\rho_{NS}(r)$ is given by

$$\rho_{NS}^{\mathrm{tunn}}(r) = \frac{N}{2\sqrt{2}\pi}\frac{G_1G_2}{G_1+G_2}\frac{1}{r^{5/4}\sqrt{(r_0-2)\sqrt{r}+r_0}}, \tag{18}$$

where $G_j=N_jT_j$ and, $r_0=4G_1G_2/(G_1+G_2)^2$. Note that Eq. (18) displays a $r^{-5/4}$ singularity when r is close to zero. This result agrees with the zero-energy limit of the Andreev reflection eingenvalue density obtained in Ref. 10 for double-tunnel junction. The main qualitatively difference between Eq. (18) and Eq. (16) is the absence of the inverse square-root singularity at $r=1$ in Eq. (18).

In order to examine in more detail the rise of the singularity at $r=1$, we consider a quantum dot coupled to two reservoirs (a normal metal and a superconductor) via an ideal contact and a barrier of arbitrary transparency. The main result of this section is the nonzero value of the density of Andreev reflection eigenvalues close to $x=0$ [$\nu_{NS}(0)\neq 0$] as we vary the barrier transparency. We shall see that $\nu_{NS}(0)$ may be used as an order parameter to the quantum transition described in Ref. 11. In circuit theory this system is described by setting $T_1=1$ and $T_2=T$ in Eq. (13), which factorizes so that the physical root is obtained from the following cubic equation:

$$(1-T)\xi^3 + [(1+a)T-1]\eta\xi^2 + (1+aT)\xi - \eta = 0. \tag{19}$$

Substituting the physical root in Eq. (14) and inserting $g_{NS}(\varepsilon)$ into Eq. (6) we obtain the density $\nu(x)$.

In Fig. 1, we show the density $\nu_{NS}(x)$ for several values of the barriers' transparency. We observe that $\nu_{NS}(0)=0$ for $T\leq 0.5$ and $\nu_{NS}(0)>0$ for $0.5<T\leq 1$. In this case $\nu_{NS}(0)$ is similar to an order parameter of a second-order phase transition. This order parameter signals the appearance of Fabry-Perot modes inside the cavity as pointed out in Ref. 11. The emergence of Fabry-Perot modes inside the dot are connected to the observation of the reflectionless tunneling regime in double-barrier NS structures. From the analytical solution, we find the behavior of $\nu_{NS}(0)$ as a function of T

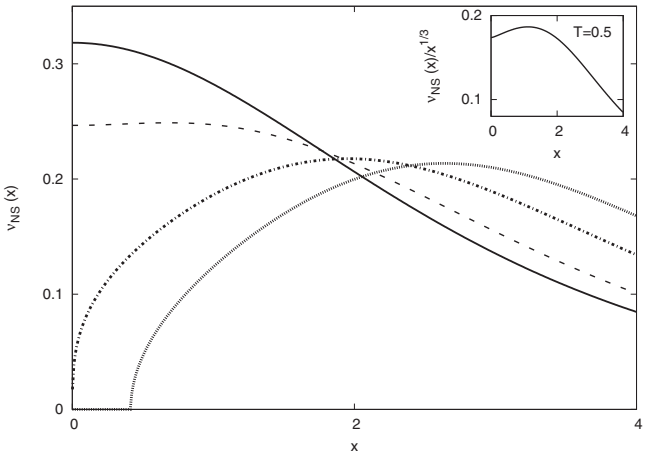

FIG. 1. Level density $\nu_{NS}(x)$ for $T_1=1$ and $T_2=1$ (full line), $T_2=0.8$ (dashed line), $T_2=0.5$ (dashed-dotted line), and $T_2=0.3$ (dotted line). The inset shows the behavior of $\nu_{NS}(x)$ divided by $x^{1/3}$ for $T_2=0.5$.

$$\nu_{NS}(0) = \frac{N_2}{\pi}\mathrm{Re}\left\{\frac{\sqrt{(a+1)T-1}}{a}\right\}. \tag{20}$$

This coincides with the result obtained for the NN case (two normal leads) discussed in Ref. 11 after it is divided by a factor 2. We also investigated the behavior of $\nu_{NS}(x)$ when x is close to zero for $T=0.5$ (see inset of Fig. 1), a 1/3 power-law behavior was obtained through analysis of Fig. 1

$$\nu_{NS}(x) \propto x^{1/3}, \quad x \to 0. \tag{21}$$

This same power-law behavior was found in Ref. 11 for two normal leads. In the next section we shall fully explore the advantage of the circuit-theory approach and describe the transition line in the T_1T_2 plane. We will also show that the first three FCS cumulants exhibit signatures of the transition as one crosses the transition lines.

IV. QUANTUM TRANSITION AND FCS CUMULANTS

In this section we consider the general case of arbitrary transmission coefficients T_1 and T_2, and investigate possible signatures of the quantum transition in the average NS cumulants. We also show that the regularizing property of $\nu_{NS}(0)$, which can be interpreted as the density of Fabry-Perot-like modes, is preserved in the general case showing that it can be used as an indicator of the onset of the reflectionless tunneling regime in the system. In order to simplify our analysis we introduce the following auxiliary variables $\zeta=T_2(1+T_1)/T_1$ and $\zeta_0=(1+T_1)/(1-T_1)$. We shall consider the general case of asymmetric barriers ($N_1 \neq N_2$). As shown in the previous section the analysis starts by solving the quartic equation given by Eq. (13).

A simple procedure to compute the cumulants is to power expand $g_{NS}(\varepsilon)$ about $\varepsilon=0$ and extract the value of the cumulants from the expansion coefficients. Inserting the pertubative expansion

$$\xi_{\pm} = A \pm B\varepsilon + C\varepsilon^2 \pm D\varepsilon^3 + E\varepsilon^4 \pm F\varepsilon^5 \ldots \tag{22}$$

and

$$\eta_{\pm} = 1 \mp \varepsilon + \frac{1}{2}\varepsilon^2 \mp \frac{1}{2}\varepsilon^3 + \frac{3}{8}\varepsilon^4 \mp \frac{3}{8}\varepsilon^5 \ldots \tag{23}$$

into Eq. (13) one can show that the coefficient A is obtained by solving the following quartic equation:

$$T_1(1-T_2)A^4 + aT_2(2-T_1)A^3 + (1+2a)$$

$$T_1T_2A^2 + a(2-T_1)T_2A - T_1 = 0. \tag{24}$$

The coefficient B can be written in terms of A as follows:

$$B = \frac{T_1A\{[(2+a)T_2-2]A^2 - 2 - aT_2\}}{4\sigma_1A^3 + 3\sigma_2^-A^2 + 2T_1T_2(1+2a)A + \sigma_2^-}, \tag{25}$$

where $\sigma_1=T_1(1-T_2)$ and $\sigma_2^-=aT_2(2-T_1)$. In the Appendix we provide explicit expressions for the higher-order expansion coefficients C, D, E, and F. Substituting Eq. (22) into $g_{NS}(\varepsilon)$, Eq. (14), we find the following power expansion:

$$g_{NS}(\varepsilon) = \alpha_0 + \alpha_1\varepsilon^2 + \alpha_2\varepsilon^4 + \ldots, \tag{26}$$

where the coefficients α_0, α_1, and α_2 are shown in the Appendix. The first three cumulants, obtained from Eq. (5) are given in terms of such coefficients as follows:

$$g_{NS} = 2q_1 = 2\alpha_0, \tag{27}$$

$$P_{NS} = 4q_2 = -4\alpha_1, \tag{28}$$

and

$$C_{NS} = q_3 = 2\alpha_2 - \alpha_1. \tag{29}$$

In Fig. 2, we show the behavior of the first three cumulants for $T_1=0.1$. In the top panels we have the NS resistance (left panel), R_{NS} (solid line), as function of the inverse of the second barrier, and the NS conductance (right panel), G_{NS} $(=1/R_{NS})$ (solid line) as function of the auxiliary parameter ζ. In the bottom panels the NS power shot-noise power (left panel), P_{NS}, and the third cumulant (right panel), C_{NS}, are shown as a function of ζ. The corresponding observables of the NN case (dashed lines) are also shown for comparison. The vertical dashed line at $\zeta=1$ serve as a "guide to the eye" to identify the change in behavior of the NS cumulants when Fabry-Perot modes appear in the system. As discussed in Ref. 11 $\zeta=1$ defines a transition line in the $T_1 \times T_2$ diagram. The minimum in the NS resistance signals a gradual transition between the reflectionless tunneling regime and the usual two-particle tunneling regime which occur at normal superconductor interfaces. In the reflectionless regime one of the quasiparticles of Andreev's process tunnels the entire sample without suffering reflection. Therefore a transport process which in principle involves two particles is effectively converted into a one-particle process. We point out the interesting behaviors of the second and third cumulants near the point $\zeta=1$. The results plotted in Fig. 2 show an increasing sensitivity of higher-order cumulants to the quantum transition in doubled-barrier dots.

We have also calculated the second and third cumulants using a numerical implementation of the scattering matrix approach. The ensemble is constructed by combining the

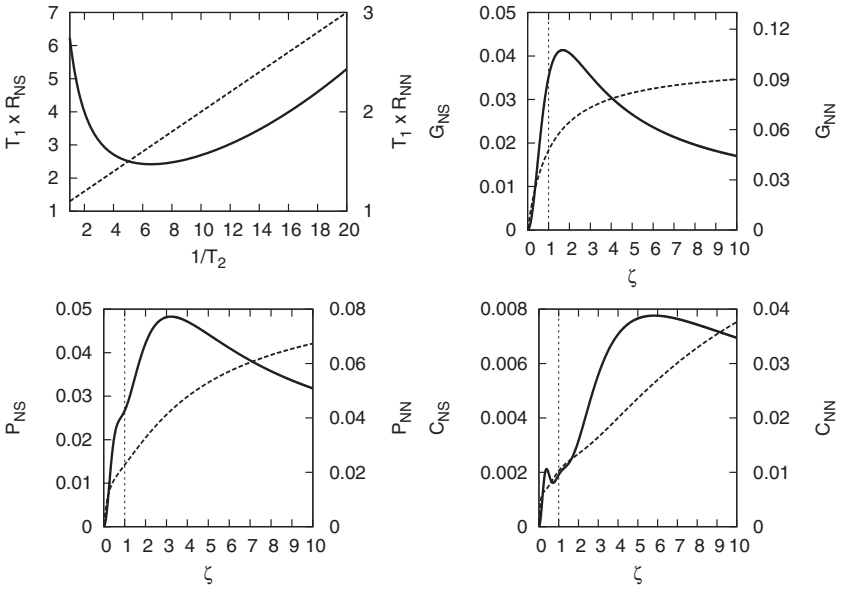

FIG. 2. The first three NS cumulants (solid lines) are shown in comparison with the normal cumulants (dashed lines), with $T_1=0.1$. The right vertical axis refers to the normal observables' scales. In the top left (right) panel we show the NS resistance (conductance) as a function of the second barrier transparency. In the bottom panels we show the shot-noise power (left) and the third cumulant (right). The vertical line at $\zeta=1$ helps us to visualize the signature of the quantum transition in the NS cumulants.

fixed scattering matrix of the two barriers, which are characterized by the transmission coefficients T_1 and T_2, with a stochastic scattering matrix belonging to the Circular Orthogonal Ensemble (COE), which accounts for the chaotic scattering inside the dot. The transmission matrix $\mathbf{t}$ of whole structure is obtained and used to calculated the Andreev reflection matrix $\mathbf{s}_{he}$. In our numerical procedure we consider symmetric leads with 50 open channels, i.e., $N_1=N_2=50$, and perform the ensemble average with 1000 realizations of the random matrix $\mathbf{s}_{he}$. The numerical results are in good agreement with our analytical expressions as can be seen from Fig. 3, where we plot the shot-noise power and the third cumulant.

We point out that the scattering approach gives all quantum corrections (weak localization and higher order) while circuit theory gives only the dominant term in the expansion in inverse powers of N. Effects of these quantum corrections can be seen in Fig. 3. It is possible to calculate analytically the weak localization correction on the FCS characteristic function of a double-barrier quantum dot if we go beyond circuit theory. Possible routes include the use of diagrammatic methods[15] for integration over the unitary group and a recent extension of circuit theory which incorporates quantum corrections.[16] In Ref. 17 the authors calculated the weak-localization correction to the shot-noise power for a chaotic cavity coupled non-ideally to normal reservoirs using both methods and reported an unexpected amplification-suppression transition in the shot-noise power as we vary the number of open channels and the barriers' transparencies.

We also study the behavior of Fano factor, defined as $F_{NS}=P_{NS}/G_{NS}$, and the skewness factor $S_{NS}=C_{NS}/G_{NS}$, which are shown in Fig. 4, for several values of the first barrier transparency T_1. One can see that both factors exhibit a sharp decrease near $\zeta=1$.

Finally, we have calculated the average density $\nu_{NS}(x)$, Eq. (6) for arbitrary T_1 and T_2. In Fig. 5 the three-dimension plot of $\nu_{NS}(x)$ at $x=0$ as a function of barriers transparencies

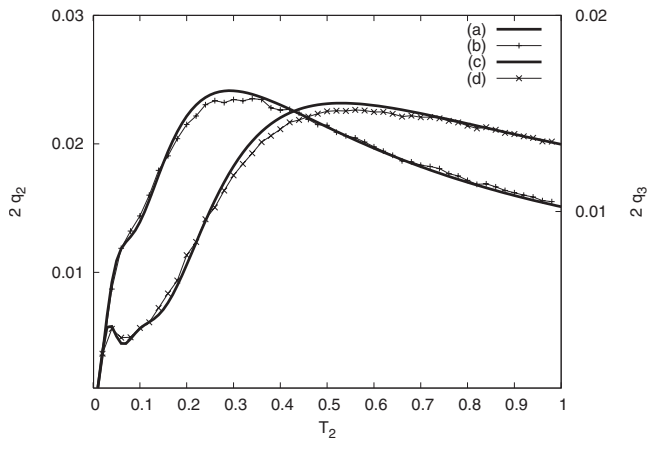

FIG. 3. Comparison between analytical results obtained from circuit theory [solid curves (a) and (c)] and numerical simulations [curves (b) and (d)] using an ensemble of scattering matrices for the second and third cumulants for $T_1=0.1$. The left vertical axis corresponds to the shot-noise power plots [(a) and (b)], while the right vertical axis corresponds to the third cumulant.

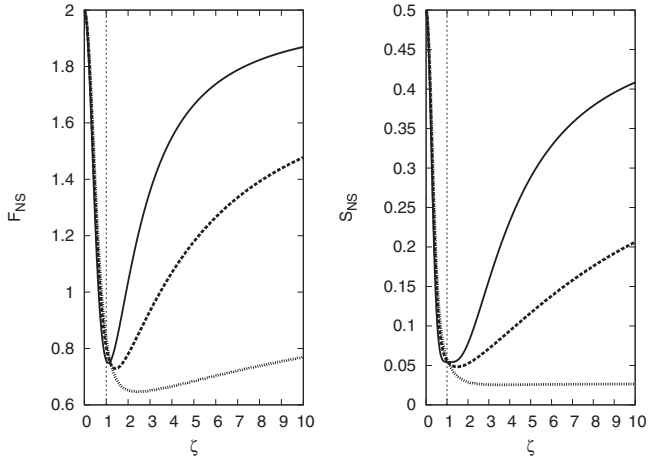

FIG. 4. Fano factor (left panel) and skewness (right panel) for $T_1=0.1$ (solid line), 0.4 (dashed line), and 0.8 (dotted line).

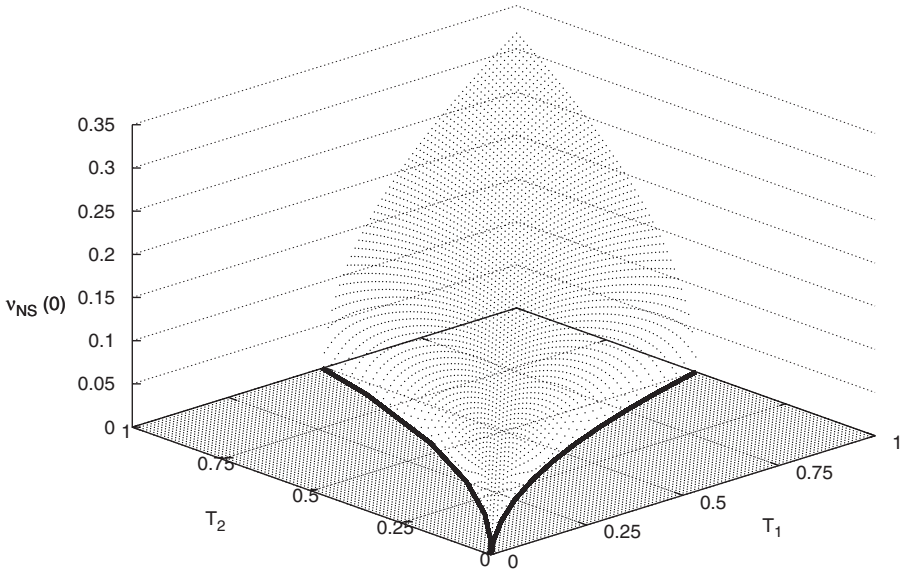

FIG. 5. Average density of Andreev reflection eigenvalues at $x=0$ as a function of the transparencies of the barriers. In the T_1T_2 plane we recover the phase diagram for the quantum transition. The solids lines correspond to the lines $\zeta=\zeta_0$ and $\zeta=1$.

T_1, and T_2 is shown. We observe that the lines $\zeta=1$ and $\zeta=\zeta_0$ delimit the region where $\nu_{NS}(0)\neq 0$, indicating that it may have the role of an order parameter, in agreement with the results of Ref. 11 for NN systems.

In terms of ζ and ζ_0 we can write $\nu_{NS}(0)$ as follows:

$$\nu_{NS}(0)=\frac{N}{\pi}\begin{cases}\frac{\sqrt{\zeta_0(\zeta-1)(\zeta_0-\zeta)}}{\zeta+\zeta_0}; & 0<\zeta<\zeta_0\\ 0; & \text{otherwise.}\end{cases} \tag{30}$$

This expression coincides with the one obtained in Ref. 11 for NN systems if the latter is divided by a factor 2.

V. SUMMARY AND CONCLUSIONS

In this work we studied the full counting statistics (FCS) of charge-transfer events of a quantum dot connected to a normal metal and a superconducting reservoir via barriers of arbitrary transparencies using the scalar version of quantum circuit theory. We started extending the scheme presented in Ref. 14 to calculate the FCS generating function of NS hybrid systems. The charge transmission events in an NS system are controlled by Andreev reflection eigenvalues, r_n, which in the absence of an external magnetic field and in the low-energy regime can be expressed in terms of the transmission eigenvalues, τ_n, of a similar NN system obtained by replacing the superconducting reservoir by a normal one. Through a careful analysis of the Andreev reflection eigenvalue density, $\rho_{NS}(r)$, we observed a gradual transition between the reflectionless tunneling regime and the standard tunneling regime in NS hybrid structures. This crossover is a consequence of a quantum transition taken place at the quantum dot, which is related to the formation of Fabry-Perot modes inside the cavity.[11] The regularized density, $\nu_{NS}(x)$, near $x=0$ $(r=1)$ can be used as an order parameter of this quantum transition. The NS charge-transfer cumulants (see Fig. 2) reveal a strong sensitivity to the position of the transitions lines discussed in Ref. 11, which contrasts with the insensitivity of the charge-transfer cumulants in the normal case. All results were compared with numerical simulations obtained from the scattering matrix formalism. Differently from other signatures of the quantum transition proposed in the literature, which appear as features in the tail of the transferred charge distribution[13] or induced in the Fano factor by a weak coulomb interaction, emulated by an electromagnetic environment,[12] the signals presented in this paper appear naturally in the first FCS cumulants and could in principle be measured experimentally. Recent measurements of higher-order FCS cumulants in quantum dots with tunnable barriers[18,19] show that similar experiments with NS systems may be within reach of current nanotechnology. In Ref. 20 a good review of the experimental field of hybrid structures (including NS systems) is presented. In this work the authors describe the problem of low-temperature thermoelectrical transport and discuss several experimental setups in which to study manifestations of the proximity effect.

A natural continuation of this work would be to investigate the transport properties of this system close to the transition lines when the incident electron energy is on the order of the Thouless energy. A careful analysis of regions away from the transition lines was presented in Ref. 10 with many interesting results. Another important problem is the study of FCS of a hybrid NS system in the presence of a magnetic field which breaks the time-reversal symmetry. In this case the connection between Andreev reflection eigenvalues and transmission eigenvalues of the correspondent normal system is no longer valid and we must work with the whole scattering matrix of the cavity.

ACKNOWLEDGMENTS

We thank S. Rodríguez-Pérez for useful discussions and help in the implementation of numerical routines. This work was partially supported by CNPq and FACEPE (Brazilian Agencies).

APPENDIX: EXPANSION COEFFICIENTS

In Sec. III we obtained the following power-series expansion for $g_{NS}(\varepsilon)$, Eq. (26):

$$g_{NS}(\varepsilon) = \alpha_0 + \alpha_1\varepsilon^2 + \alpha_2\varepsilon^4 + \ldots . \tag{A1}$$

Here we present the expansion coefficients (α_0, α_1, and α_2) in terms of the expansion coefficients of the roots $\xi_{\pm}$, shown in Eq. (22). We get

$$\alpha_0 = NT_2(1 - tA^2)J^2B, \tag{A2}$$

where $J=(1+tA^2)^{-1}$, and $t=1-T_2$,

$$\alpha_1 = \frac{NT_2J^4}{2}[-t^3[(B-2D)A^6 + 4CBA^5] - t^2[(-2tB^3 + B - 3D)A^4 - 8CBA^3] + t\{[(1-12t)B - 2D]A^2 + 12CBA\} + 2(tB^2+1)B - 2D], \tag{A3}$$

$$\alpha_2 = \frac{NT_2J^6}{8}[-t^5\{(B+4D-8F)A^3 - 8[(B-2D)C - 2BE]A^2 + 32CB^3\}A^7 + t^4[24t(-4B^2 + DB + C^2)B - 3(B+4D-8F)]A^8 + 2t^3((4t\{tB^4 - 2[6(C^2+DB) - 8B^2]\}B - B - 4D + 8F)A - 24[-6tCB^3 + CB - 2(BE+CD)])A^5 - 2t^2\{20t[3tB^3 + 6(DB+C^2) - B^2]B - B - 4D + 8F\}A^4 - 32t^2\{-5tB^3C + 2[(C-2E)B - 2CD]\}A^3 + t\{8t[15B^4 + 2B^2 - 12(C^2+DB)]B + 3(B+4D-8F)\}A^2 + 8t\{-20tB^3C + 3[B(2E-C) + 2CD]\}A - \{4t[tB^4 + (B-6D)B - 6C^2]B - B - 4D + 8F\}]. \tag{A4}$$

The variables C, D, E, and F are presented below in terms of the following variables: $\sigma_1=(1-T_2)T_1$, $\sigma_2^{\pm}=(2\pm T_1)aT_2$, $\sigma_3=(1+2a)T_1T_2$, and $\sigma_4=(1+aT_2)T_1$, $\gamma=[4\sigma_1A^3+3\sigma_2^-A^2+2T_1T_2(1+2a)A+\sigma_2^-]^{-1}$

$$C = -\frac{\gamma}{2}\{[\sigma_2^+ - 4\sigma_1(2B+1)]A^3 + 12[\sigma_1(B+1) - aT_2]BA^2 + [2(3\sigma_2^-B - 2\sigma_3)B - (4+3aT_2)T_1 + 2aT_2]A + 2[\sigma_3B + 2(\sigma_4 - aT_2)]B\} \tag{A5}$$

$$D = -\frac{\gamma}{2}[[4\sigma_1(B-2C+1) - \sigma_2^+]A^3 + 12\{\sigma_1[(2C-B-1)B + C] + aT_2(B-C)\}A^2 + \{4[\sigma_1(2B+3) - aT_2]B^2 + 12\sigma_2^-T_1T_2CB + 2\sigma_3(B-2C) + (4+3aT_2)T_1 - 2aT_2\}A + 2[(\sigma_2^- - \sigma_3 - B)B + 2(\sigma_3 - \sigma_4 + aT_2)]B + 4(\sigma_4 - aT_2)C] \tag{A6}$$

$$E = -\frac{\gamma}{8}[[16\sigma_1(C-B-2D-1) + (10+3T_1)aT_2]A^3 + 24(\sigma_1\{[B+4(D-C)+2]B + 2C^2\} + 2(\sigma_1 - aT_2)(D-C) - 48aT_2B)A^2 + (8\{-4\sigma_1B^2 + 6[\sigma_1(2C-1) + aT_2]B + 12(\sigma_1 - aT_2)C + 6\sigma_2^-D - \sigma_3\}B + 24\sigma_2^-C^2 + 8\sigma_3C - 16\sigma_3D - (16+13aT_2)T_1 + 10aT_2)A + 4\{2\sigma_1B^4 + 4(\sigma_1 - aT_2)B^3 + (6\sigma_2^-C + \sigma_3)B^2 + 4[\sigma_3(D-C) + \sigma_4 - aT_2]B + 2\sigma_3C^2\} + 4(aT_2 - \sigma_4)(C-D)] \tag{A7}$$

$$F = -\frac{\gamma}{8}[\{4\sigma_1[3B + 4(D-C-2E+1)] - (10+3T_1)aT_2\}A^3 + (24\sigma_1\{-B^2 + 2[C - 2(D-E) - 1]\}B + 48\{[aT_2B - \sigma_1C(C+2D)] + (C-D+E)(\sigma_1 - aT_2)\})A^2 + (16\sigma_1B^3 + 48[2\sigma_1(D-C) + (\sigma_1 - aT_2)]B^2 + 6\{16[\sigma_1C^2 + (\sigma_1 - aT_2)(D-C)] + 8\sigma_2^-E + \sigma_3\}B + 48[(\sigma_1 - aT_2)C^2 + \sigma_2^-D] + 8\sigma_3(D-C-2E))A - 4\{-2\sigma_1B^4 + 4[\sigma_1(2C-1) + aT_2]B^3 + [12(\sigma_1 - aT_2)C + 6\sigma_2^-D - \sigma_3]B^2 + 2\{3\sigma_2^-C^2 + \sigma_3[C - 2(D-E)] - 2(\sigma_4 - aT_2)\}B + 2\{\sigma_4[2(D+1) - C] - 2T_2\}C - 8(\sigma_4 - aT_2)(D-E)\}] \tag{A8}$$

The coefficients A and B are given by Eq. (24) and Eq. (25), respectively, for the most general case presented in Sec. IV. With α_0, α_1, and α_2 we can compute the first three cumulants analytically through Eqs. (27)–(29). The behavior of such cumulants as we vary the barriers transparencies are shown in Fig. 2.

[1] A. F. Andreev, Zh. Eksp. Teor. Fiz. **46**, 1823 (1964) [Sov. Phys. JETP **19**, 1228 (1964)].
[2] L. S. Levitov and G. B. Lesovik, Pis'ma Zh. Eksp. Teor. Fiz. **58**, 225 (1993) [JETP Lett. **58**, 230 (1993)].
[3] Yu. V. Nazarov, in *Handbook of Theoretical and Computational Nanotechnology*, edited by M. Rieth and W. Schommers (American Scientific Publishers, Stevenson Ranch, CA, 2006).
[4] C. W. J. Beenakker, Phys. Rev. B **46**, 12841 (1992).
[5] C. W. J. Beenakker, in *Mesoscopic Quantum Physics*, edited by E. Akkermans, G. Montambaux, and J.-L. Pichard, Lectures at the Les Houches Summer School Vol. 61 (North-Holland, Amsterdam, 1994).
[6] Yu. V. Nazarov, Phys. Rev. Lett. **73**, 134 (1994).
[7] J. A. Melsen and C. W. J. Beenakker, Physica B **203**, 219 (1994).
[8] Yu. V. Nazarov, in *Quantum Dynamics of Submicron Structures*, edited by H. A. Cerdeira, B. Kramer, and G. Schön (Kluwer, Dordrecht, 1995), p. 687; Yu. V. Nazarov, Superlattices Microstruct. **25**, 1221 (1999).
[9] M. Vanević and W. Belzig, Phys. Rev. B **72**, 134522 (2005).
[10] P. Samuelsson, W. Belzig, and Yu. V. Nazarov, Phys. Rev. Lett. **92**, 196807 (2004).
[11] A. M. S. Macêdo and A. M. C. Souza, Phys. Rev. E **71**, 066218 (2005).
[12] A. M. S. Macêdo and A. M. C. Souza, Phys. Rev. B **72**, 165340 (2005).
[13] A. L. R. Barbosa, A. F. Macedo-Junior, and A. M. S. Macêdo, Phys. Rev. B **78**, 045306 (2008).
[14] G. C. Duarte-Filho, A. F. Macedo-Junior, and A. M. S. Macêdo, Phys. Rev. B **76**, 075342 (2007).
[15] P. W. Brouwer and C. W. J. Beenakker, J. Math. Phys. **37**, 4904 (1996).
[16] G. Campagnano and Yu. V. Nazarov, Phys. Rev. B **74**, 125307 (2006).
[17] J. G. G. S. Ramos, A. L. R. Barbosa, and A. M. S. Macêdo, Phys. Rev. B **78**, 235305 (2008).
[18] S. Gustavsson, R. Leturcq, B. Simovič, R. Schleser, T. Ihn, P. Studerus, K. Ensslin, D. C. Driscoll, and A. C. Gossard, Phys. Rev. Lett. **96**, 076605 (2006).
[19] S. Gustavsson, R. Leturcq, T. Ihn, K. Ensslin, M. Reinwald, and W. Wegscheider, Phys. Rev. B **75**, 075314 (2007).
[20] F. Giazotto, T. T. Heikkilä, A. Luukanen, A. M. Savin, and J. P. Pekola, Rev. Mod. Phys. **78**, 217 (2006).